

Structures, Energetics, and Spectra of $\text{Cl}^-(\text{H}_2\text{O})_n$ Clusters, $n = 1-6$: Ab Initio Study

M. Masamura*

Department of Preventive Dentistry, Okayama University Dental School, Shikata-cho 2-5-1, Okayama, 700-8525 Japan

Received: December 31, 2001; In Final Form: April 8, 2002

$\text{Cl}^-(\text{H}_2\text{O})_n$ ($n = 1-6$) clusters have been studied using ab initio calculations. The structures of the various $\text{Cl}^-(\text{H}_2\text{O})_n$ isomers differed considerably from those of the corresponding $\text{F}^-(\text{H}_2\text{O})_n$ isomers for $n = 2$ and $4-6$, and especially so for $n = 6$. The relative stability of the $\text{Cl}^-(\text{H}_2\text{O})_n$ isomers is also much different from that of the corresponding $\text{F}^-(\text{H}_2\text{O})_n$ isomers at 0 and 298 K. The relative stability of the $\text{Cl}^-(\text{H}_2\text{O})_n$ isomers at 298 K is different from that at 0 K, because of the entropy effect. The ionization potential, charge-transfer-to-solvent (CTTS) energy, and the OH stretching vibrational spectra are reported to facilitate future experimental work.

I. Introduction

The hydration of ions is a subject of interest in solute and biochemistry.¹ The structures of aqua-halide anion clusters in regard to the internal or surface state of the halide anion have long been the subject of controversy.²⁻²² The various structures of the $\text{F}^-(\text{H}_2\text{O})_n$ cluster (where $n = 1-6$) have been examined using MP2/6-311++G(d,p) and BLYP/6-311++G(d,p) calculations,²³ and the various structures of $\text{I}^-(\text{H}_2\text{O})_n$ for $n = 1-6$ have also been examined using extensive ab initio calculations.²⁴ For $\text{Cl}^-(\text{H}_2\text{O})_n$, the structures that water molecules form around the chloride ion (Cl^-) in gas-phase clusters reflect the competition between solvation of the ion vs. hydrogen bonding among the water molecules. If hydrogen bonding to the ion dominates, then the Cl^- ion will move to the interior of a solvation shell. If hydrogen bonding among the waters dominates, then the Cl^- ion will move to the surface of a neutral water cluster.²⁵ Molecular dynamics²⁶⁻³⁸ and ab initio calculations^{4,5,10,39-41} both predict that the surface states dominate in $\text{Cl}^-(\text{H}_2\text{O})_n$ clusters, even for large values of n . However, the effects of temperature and of the zero-point energy maintain the possibility of interior structures.^{4,8,31,36,37}

Reference 41 contains the most extensive ab initio study on $\text{Cl}^-(\text{H}_2\text{O})_n$. However, the structures of only the most stable isomers for $\text{Cl}^-(\text{H}_2\text{O})_n$ ($n = 1-6$) at 0 K were discussed. Therefore, the various low-lying energy structures of $\text{Cl}^-(\text{H}_2\text{O})_n$ were calculated using ab initio methods in the present work. The available experimental results can be grouped into three sets of data: formation enthalpies,⁴²⁻⁴⁴ photodetachment energies,^{3,40} and vibrational spectra.²⁵

The purpose of this paper is (1) to show that the structures of the various $\text{Cl}^-(\text{H}_2\text{O})_n$ isomers differ considerably from those of the corresponding $\text{F}^-(\text{H}_2\text{O})_n$ isomers for $n = 2$ and $4-6$, and especially so for $n = 6$; (2) to show that the relative stability of the $\text{Cl}^-(\text{H}_2\text{O})_n$ isomers is significantly different from that of the corresponding $\text{F}^-(\text{H}_2\text{O})_n$ isomers at 0 and 298 K; (3) to show that the relative stability of the $\text{Cl}^-(\text{H}_2\text{O})_n$ isomers at 298 K is markedly different from that at 0 K owing to the entropy effect;

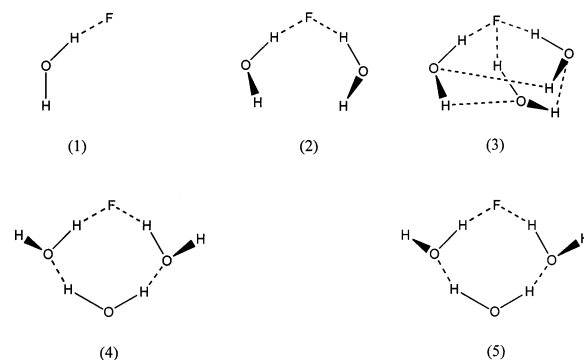


Figure 1. Sketches of the optimized structures of $\text{F}^-(\text{H}_2\text{O})_n$ ($n = 1-3$). (4) to calculate the ionization potentials (IPs); and (5) to calculate the OH stretching infrared (IR) spectra.

II. Computation Methods

We used the Gaussian 94⁴⁵ and Gaussian 98⁴⁶ programs, operating on the SX-5, VPP5000, and SGI2800 computers located at the Research Center for Computational Science.

For $\text{F}^-(\text{H}_2\text{O})_n$ ($n = 1-4$), we considered the isomers discussed in ref 47 (see Figures 1 and 2). For $\text{F}^-(\text{H}_2\text{O})_n$ ($n = 5$ and 6), we considered the isomers discussed in ref 23 (see Figures 3 and 4). For $\text{Cl}^-(\text{H}_2\text{O})_n$ ($n = 1-6$), we substituted Cl for F in the above structures, and then optimized the resulting structures. Also, we optimized the structures of the isomers discussed in ref 41, (28') and (29') (see Figures 5-8).

MP2/aug-cc-pVDZ calculations could not be carried out owing to the large CPU time required. Therefore, we carried out full geometry optimizations using the MP2/6-31++G(2d,2p) method for $\text{Cl}^-(\text{H}_2\text{O})_n$ ($n = 1-6$). We also performed vibrational analysis for all of the clusters having the optimized structures to confirm that all of the vibrational frequencies are real. Also, we calculated the energies of those isomers at the MP4SDTQ/6-311++G(2d,2p)/MP2/6-31++G(2d,2p) levels. The zero-point energies were evaluated at the MP2/6-31++G(2d,2p) level. The core electrons were frozen, and for the reason described in ref 48, the keyword "VeryTight" in the Gaussian 94 and Gaussian 98 programs was not used, i.e., standard optimization convergence criteria were used.

* E-mail address: tokin@mx3.tiki.ne.jp. Fax number: 81-86-235-6714. Telephone: 81-86-235-6712.

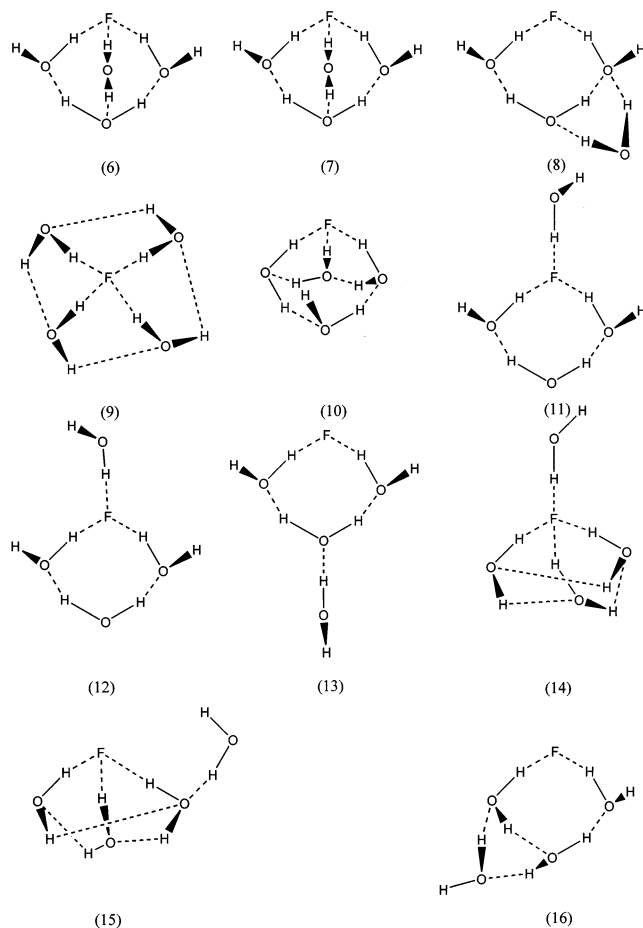


Figure 2. Sketches of the optimized structures of $F^-(H_2O)_4$.

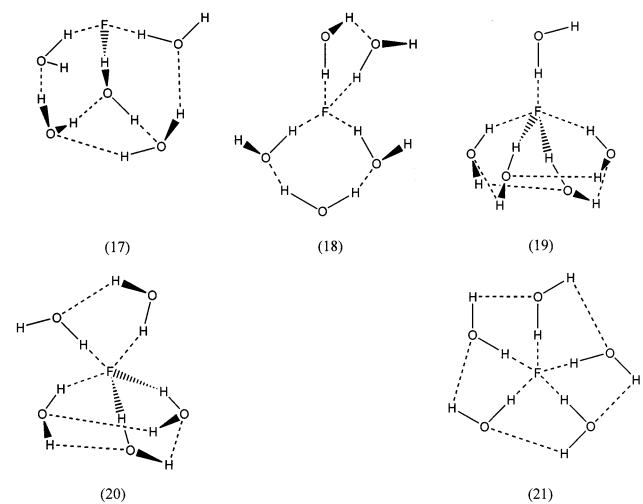


Figure 3. Sketches of the optimized structures of $F^-(H_2O)_5$.

The conversion of the computed energies to enthalpies for comparison with experimental data was represented by

$$\Delta H^{298K} = \Delta E_e^{\circ} + \Delta E_v^{\circ} + \Delta(\Delta E_v^{298K}) + \Delta E_r^{298K} + \Delta E_t^{298K} + \Delta(PV)$$

where ΔE_e° is the electronic energy change, ΔE_v° is the change in the zero-point energy, $\Delta(\Delta E_v^{298K})$ is the vibrational energy change for the thermodynamic path from 0 to 298 K, and the remaining quantities are for the changes in rotational and translational energy, and for the work term, which were treated

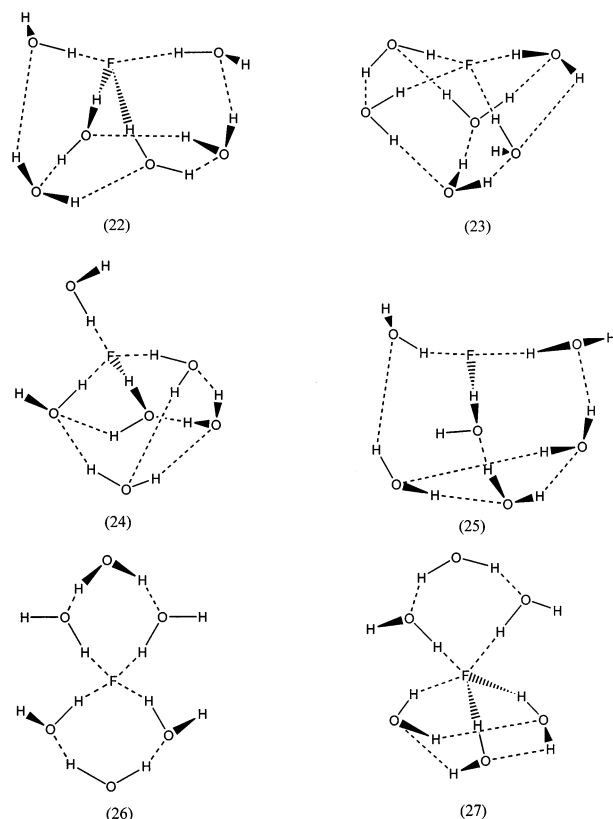


Figure 4. Sketches of the optimized structures of $F^-(H_2O)_6$.

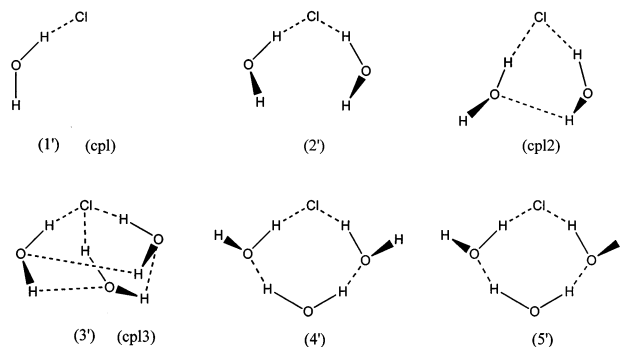


Figure 5. Sketches of the optimized structures of $Cl^-(H_2O)_n$ ($n = 1-3$). The isomers (cpl2) and (cpl3) are the isomers from ref 41.

classically. The enthalpy change of $Cl^-(H_2O)_n$ ($\Delta H_{n-1,n}^{298K}$) was calculated using the following formula:

$$\Delta H_{n-1,n}^{298K} = H(Cl^-(H_2O)_n) - H(Cl^-(H_2O)_{n-1}) - H(H_2O)$$

Thermal corrections were evaluated using the MP2/6-31++G-(2d,2p) results. The basis set superposition error (BSSE) was corrected using the counterpoise method.^{49,50}

For $Cl^-(H_2O)$, when the basis set is smaller, the counterpoise-uncorrected intermolecular interaction energies are closer to the CBS limit than the counterpoise-corrected intermolecular interaction energies at the MP2 and MP4 levels (Figure 9).⁵¹ Also, the counterpoise-uncorrected $-\Delta H_{n-1,n}^{298K}$ are more reliable than the counterpoise-corrected $-\Delta H_{n-1,n}^{298K}$ evaluated at the MP2/6-31++G(2d,2p) level for $CH_3S^-(H_2O)_n$ ($n = 1-3$).⁵² A similar trend was found for $F^-(H_2O)_n$ ($n = 1-6$).²³ Therefore, we used the counterpoise-uncorrected $-\Delta H_{n-1,n}^{298K}$ evaluated at the MP4/6-311++G(2d,2p)//MP2/6-31++G(2d,2p) level.

When certain frequencies are very low ($< 10 \text{ cm}^{-1}$), a serious error in the Gibbs free energy can arise owing to an overesti-

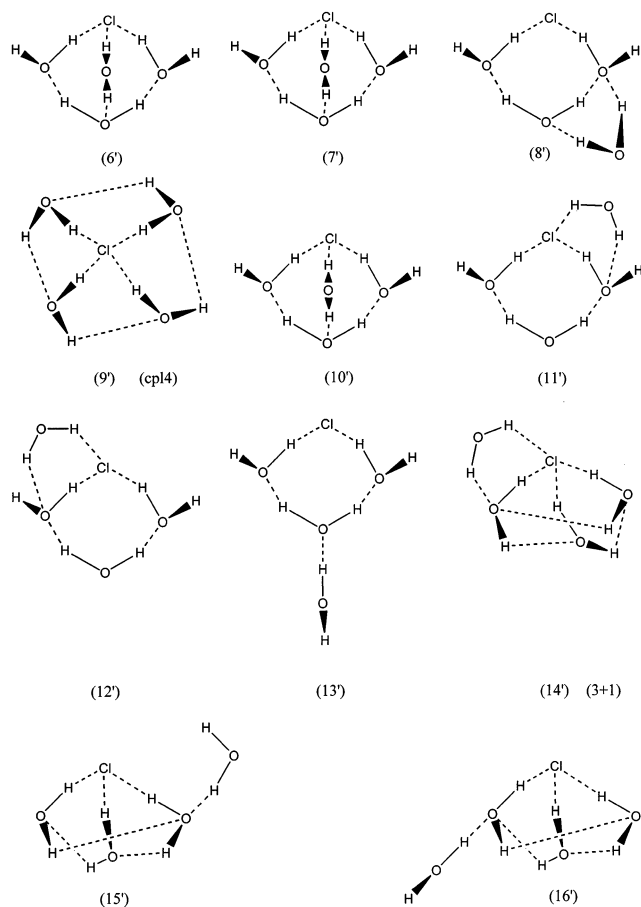


Figure 6. Sketches of the optimized structures of $\text{Cl}^-(\text{H}_2\text{O})_4$. Isomer (cpl4) is the isomer from ref 41 and isomer (3 + 1) is the isomer from ref 10.

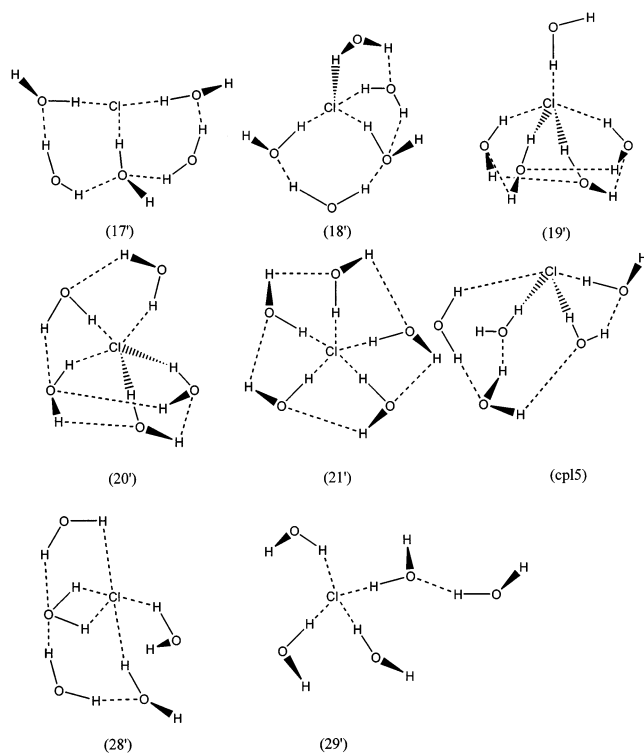


Figure 7. Sketches of the optimized structures of $\text{Cl}^-(\text{H}_2\text{O})_5$. Isomer (cpl5) is the isomer from ref 41.

mated entropy corresponding to these low frequencies.²⁴ However, for our $\text{Cl}^-(\text{H}_2\text{O})_n$ calculations, no such error arose.

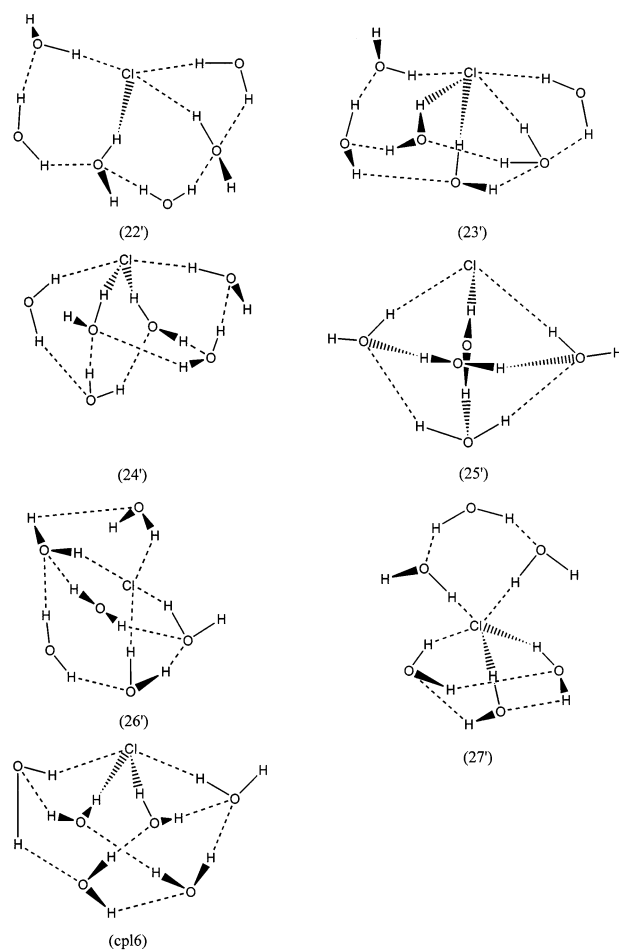


Figure 8. Sketches of the optimized structures of $\text{Cl}^-(\text{H}_2\text{O})_6$. Isomer (cpl6) is the isomer from ref 41.

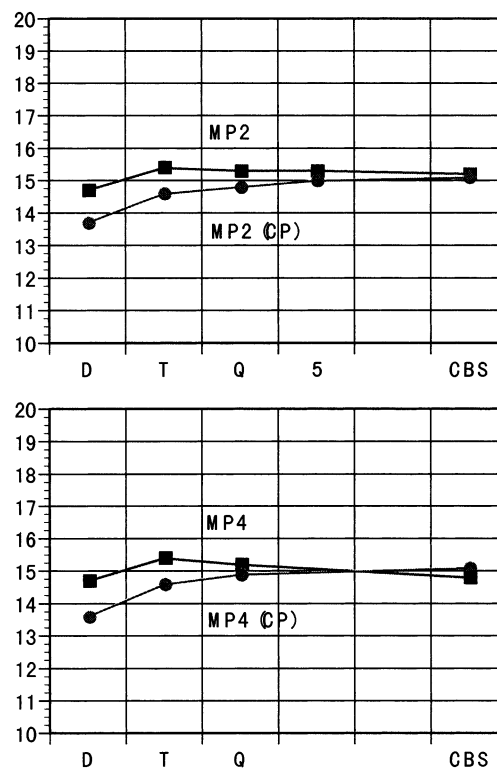


Figure 9. Calculated intermolecular interaction energies of $\text{Cl}^-(\text{H}_2\text{O})$ as a function of the correlation consistent basis set (aug-cc-pVxZ ($x = \text{D, T, Q, 5}$)) used. The counterpoise-corrected values are denoted by CP. The complete basis set (CBS) limit was estimated based on ref 55.

TABLE 1: Calculated Energies of the $\text{Cl}^-(\text{H}_2\text{O})_n$ ($n = 0-6$) Clusters^a

n	isomer	MP2/6-31++G(2d,2p)	MP4/6-311++G(2d,2p)
0		-459.69791	-459.74752
1	1'	-535.98541	-536.08140
2	cp12	-612.27327	-612.41533
	2'	-612.27242	-612.41475
3	3'	-688.56251	-688.75078
	4'	-688.55913	-688.74704
	5'	-688.55947	-688.74740
4	6'	-764.84334	-765.07719
	7'	-764.84744	-765.08141
	8'	-764.84200	-765.07571
	9'	-764.84911	-765.08294
	10'	-764.84766	-765.08167
	11'	-764.84249	-765.07640
	12'	-764.84300	-765.07694
	13'	-764.84201	-765.07509
	14'	-764.84504	-765.07924
	15'	-764.84378	-765.07751
	16'	-764.84314	-765.07684
5	cp15	-841.13190	-841.41187
	17'	-841.12612	-841.40587
	18'	-841.12867	-841.40861
	19'	-841.12898	-841.40861
	20'	-841.12785	-841.40776
	21'	-841.12913	-841.40808
	28'	-841.12951	-841.40939
	29'	-841.12923	-841.40857
6	cp16	-917.42016	-917.74563
	22'	-917.40683	-917.73252
	23'	-917.41456	-917.74013
	24'	-917.41553	-917.74077
	25'	-917.41534	-917.74082
	26'	-917.41277	-917.73843
	27'	-917.40847	-917.73394

^a Eh.**TABLE 2: Reliability of MP2/6-31++G(2d,2p) and MP4/6-311++G(2d,2p) Calculations^a**

n	isomer	$-\Delta H_{n-1,n}^{298K}$ (kcal/mol)		
		MP2/ 6-31++G(2d,2p)	MP4/ 6-311++G(2d,2p)	MP2/ aug-cc-pVDZ ^b
1	1'	14.5 (13.4)	15.1 (13.3)	14.4 (13.4)
2	cp12	13.4 (12.0)	13.8 (11.9)	13.4 (12.0)
3	3'	13.9 (12.0)	14.4 (11.9)	14.2 (12.4)
	4'	12.1 (10.3)	12.4 (10.2)	12.0 (10.5)
4	9'	12.2 (10.1)	12.3 (9.5)	12.1 (10.2)
	14'	10.1 (8.8)	10.4 (8.8)	10.4 (9.0)

^a $-\Delta H_{n-1,n}^{298K}$ for the two isomers of the $n = 4$ cluster were computed with respect to isomer (3'). The numbers in parentheses indicate the BSSE-corrected values. ^b From ref 10.

According to ref 24, in the case of imaginary frequencies, the vibrational entropy, which is often treated as zero, is given by 10.5 cal/mol K.

III. Results and Discussion

The optimized $\text{Cl}^-(\text{H}_2\text{O})_n$ structures are shown in Figures 5 to 8. The initial structures of the (1'), (2'), (3'), ..., and (27') clusters are the structures from the substituted Cl for F in the (1), (2), (3), ..., and (27) isomers, respectively. All of the present clusters, except for isomer (2'), have real vibrational frequencies and correspond to the equilibrium structures. Isomer (2') is a transition state structure with one imaginary frequency. Table 1 shows the calculated energies for $\text{Cl}^-(\text{H}_2\text{O})_n$.

MP4/6-311++G(2d,2p)//MP2/6-31++G(2d,2p) calculations for $\text{SH}^-(\text{H}_2\text{O})_n$ are known to be reliable,⁵³ and therefore it is

TABLE 3: Relative Stability of Various Isomers of $\text{Cl}^-(\text{H}_2\text{O})_n$ Clusters for $n = 2-6$ at 0 and 298 K, respectively^a

n	isomer	relative energy		relative Gibbs free energy	
		MP2/6-31 ++G(2d,2p)	MP4/6-311 ++G(2d,2p)	MP2/6-31 ++G(2d,2p)	MP4/6-311 ++G(2d,2p)
2	cp12	0.0 (0.0)	0.0 (0.0)	0.0	0.0
	2'	0.5 (0.2)	0.4 (0.0)	-2.3	-2.4
3	3'	0.0 (0.0)	0.0 (0.0)	0.0	0.0
	5'	1.9 (1.3)	2.1 (1.5)	0.2	0.4
	4'	2.1 (1.4)	2.3 (1.7)	-0.2	0.0
4	9'	0.0 (0.0)	0.0 (0.0)	0.0	0.0
	10'	0.9 (0.5)	0.8 (0.4)	-0.7	-0.8
	7'	1.1 (0.7)	1.0 (0.6)	-0.4	-0.5
	14'	2.6 (1.5)	2.3 (1.2)	-0.6	-0.9
	15'	3.3 (2.3)	3.4 (2.4)	-0.5	-0.4
	6'	3.6 (2.4)	3.6 (2.4)	0.6	0.6
	16'	3.7 (2.6)	3.8 (2.7)	-0.4	-0.3
	12'	3.8 (2.2)	3.8 (2.2)	-0.9	-0.9
	11'	4.2 (2.5)	4.1 (2.4)	-0.5	-0.6
	8'	4.5 (3.2)	4.5 (3.2)	0.9	0.9
	13'	4.5 (3.0)	4.9 (3.4)	-0.2	0.2
5	cp15	0.0 (0.0)	0.0 (0.0)	0.0	0.0
	28'	1.5 (0.9)	1.6 (1.0)	-0.3	-0.2
	29'	1.7 (1.3)	2.1 (1.7)	-0.2	0.2
	21'	1.7 (1.5)	2.4 (2.2)	0.7	1.4
	19'	1.8 (0.9)	2.1 (1.2)	-2.8	-2.5
	18'	2.0 (1.2)	2.0 (1.2)	-0.4	-0.4
	20'	2.5 (1.7)	2.6 (1.8)	0.1	0.2
	17'	3.6 (2.2)	3.8 (2.4)	-0.4	-0.2
6	cp16	0.0 (0.0)	0.0 (0.0)	0.0	0.0
	24'	2.9 (1.9)	3.0 (2.0)	0.5	0.6
	25'	3.0 (2.2)	3.0 (2.2)	1.4	1.4
	23'	3.5 (2.6)	3.5 (2.6)	0.7	0.7
	26'	4.6 (3.3)	4.5 (3.2)	0.9	0.8
	27'	7.3 (5.0)	7.3 (5.0)	-1.0	-1.0
	22'	8.4 (5.6)	8.2 (5.4)	0.8	0.6

^a kcal/mol. Parentheses indicate the relative energy including the zero-point energy.

expected that MP4/6-311++G(2d,2p)//MP2/6-31++G(2d,2p) calculations for $\text{Cl}^-(\text{H}_2\text{O})_n$ are also reliable. In fact, Table 2 shows that the MP2/6-31++G(2d,2p) and MP4/6-311++G(2d,2p) results agree with the MP2/aug-cc-pVDZ results from ref 10.

Figures 1 to 8 show that the conformation of the optimized structures of the isomers for $\text{Cl}^-(\text{H}_2\text{O})_n$ is different from that of $\text{F}^-(\text{H}_2\text{O})_n$. For the isomers (cp12), (10), (10'), (11), (11'), (12), (12'), (14), (14'), (18), (18'), (20), and (20'), the conformation of the $\text{Cl}^-(\text{H}_2\text{O})_n$ isomer structures is slightly different from that of the corresponding $\text{F}^-(\text{H}_2\text{O})_n$ isomers. This is because the intermolecular interaction between Cl^- and the water molecules is much weaker than that between F^- and the water molecules. Therefore, the water molecules in $\text{Cl}^-(\text{H}_2\text{O})_n$ tend to form hydrogen bonds with the other water molecules in the cluster.

For isomers (16), (16'), (17), (17'), (cp15), (28'), (29'), (22), (22'), (23), (23'), (24), (24'), (25), (25'), (26), (26'), and (cp16), the conformation of the $\text{Cl}^-(\text{H}_2\text{O})_n$ isomers is very different from that of the corresponding $\text{F}^-(\text{H}_2\text{O})_n$ isomers. Three- and four-point hydrogen bonds are important in the stabilization of these isomers. The ionic radius of Cl^- is larger than that of F^- , and thus the position of the water molecules around Cl^- is different from those around F^- . For three-point hydrogen bonds and four-point hydrogen bonds, the intermolecular distances between water molecules are very important. As a result, the conformation in $\text{Cl}^-(\text{H}_2\text{O})_n$, where three- and four-point hydrogen bonds form, is different from that in $\text{F}^-(\text{H}_2\text{O})_n$. Thus, the conformation

TABLE 4: NBO Charge of $\text{Cl}^-(q_{\text{cl}})$, the Vertical Ionization Potential (IP), the Integral (dIP_v), and Differential (DIP_v) Shifts, and the Charge-Transfer-to-Solvent Energy (E_{CTTS}) for $\text{Cl}^-(\text{H}_2\text{O})_n$ Clusters at the MP2/6-31++G(2d,2p) Level^a

n	isomer	q_{cl}	IP _v (eV)	dIP _v (eV)	DIP _v (eV)	E_{CTTS} (eV)	expt. IP _v (eV) ^b
0		-1.00	3.46(4.09)				3.61
1	1'	-0.94	4.30(4.81)	0.84(0.72)	0.84(0.72)	5.04	4.37
2	cpl2	-0.91	4.93(5.45)	1.47(1.36)	0.63(0.64)	5.21	4.97
	2'	-0.90	4.93(5.47)	1.47(1.38)	0.63(0.66)	5.26	
3	3'	-0.90	5.38(6.06)	1.92(1.97)	0.45(0.61)	5.45	5.50
	4'	-0.88	5.39(5.95)	1.93(1.86)	0.46(0.50)	5.31	
	5'	-0.88	5.39(5.95)	1.93(1.86)	0.46(0.50)	5.33	
4	6'	-0.86	5.78(6.45)	2.32(2.46)	0.40(0.39)	5.39	5.92
	7'	-0.87	--- ^c (6.43)	--- ^c (2.34)	--- ^c (0.37)	5.47	
	8'	-0.86	5.57(6.25)	2.11(2.16)	0.19(0.19)	5.35	
	9'	-0.90	5.73(6.51)	2.27(2.42)	0.35(0.45)	5.58	
	10'	-0.87	5.73(6.45)	2.27(2.36)	0.35(0.39)	5.50	
	11'	-0.86	5.82(6.52)	2.36(2.43)	0.44(0.46)	5.46	
	12'	-0.85	5.82(6.53)	2.36(2.44)	2.36(2.44)	5.48	
	13'	-0.86	5.66(6.21)	2.20(2.12)	0.28(0.15)	5.32	
	14'	-0.88	5.91(6.61)	2.45(2.52)	0.53(0.55)	5.59	
	15'	-0.88	5.75(6.42)	2.29(2.33)	0.37(0.36)	5.48	
	16'	-0.88	5.69(6.37)	2.23(2.28)	0.31(0.31)	5.47	
5	cpl5	-0.86	6.21(6.88)	2.75(2.79)	0.48(0.37)	5.68	6.21
	17'	-0.84	6.36(6.97)	2.90(2.88)	0.63(0.46)	5.56	
	18'	-0.87	6.26(7.01)	2.80(2.92)	0.53(0.50)	5.62	
	19'	-0.89	6.28(7.03)	2.82(2.94)	0.55(0.52)	5.62	
	20'	-0.88	6.38(7.10)	2.92(3.01)	0.65(0.59)	5.70	
	21'	-0.89	6.20(6.87)	2.74(2.78)	0.47(0.36)	5.67	
	28'	-0.85	6.28(6.95)	2.82(2.86)	0.55(0.44)	5.61	
	29'	-0.88	6.06(6.84)	2.60(2.75)	0.33(0.33)	5.61	
6	cpl6	-0.85	6.42(7.07)	2.96(2.98)	0.21(0.19)	5.62	6.58
	22'	-0.83	6.82(7.45)	3.36(3.36)	0.61(0.57)	5.68	
	23'	-0.86	6.67(7.35)	3.21(3.26)	0.46(0.47)	5.77	
	24'	-0.83	6.41(7.19)	2.95(3.10)	0.20(0.31)	5.67	
	25'	-0.85	6.44(7.07)	2.98(2.98)	0.23(0.19)	5.66	
	26'	-0.84	6.55(7.27)	3.09(3.18)	0.34(0.39)	5.67	
	27'	-0.87	6.77(7.49)	3.31(3.40)	0.56(0.61)	5.71	

^a IP_v, dIP_v, DIP_v were obtained by the energy difference of the ionic and neutral species keeping the geometry unchanged, while their values in parentheses were obtained using Koopman's theorem. ^b From ref 3. ^c Values cannot be calculated.

of the $\text{Cl}^-(\text{H}_2\text{O})_n$ isomers is very different from that of the corresponding $\text{F}^-(\text{H}_2\text{O})_n$ isomers.

For $\text{Cl}^-(\text{H}_2\text{O})_n$ at 0 K, Table 3 shows that: (1) for $n = 2$, isomer (cpl2) is a local minima, and isomer (2') is a transition state structure, only being 0.4 kcal/mol above the local minimum energy; (2) for $n = 3$, isomer (3') is the most stable isomer, and isomers (4') and (5') are less stable than isomer (3') by 2 kcal/mol. The stability of isomer (4') is close to that of isomer (5'); (3) for $n = 4$, isomer (9') surface structure is the most stable, with isomer (10') surface structure being less stable than isomer (9') by 0.8 kcal/mol. Isomer (7') surface structure is less stable than isomer (10') by only 0.2 kcal/mol. The other isomers are considerably less stable than isomer (7'); (4) for $n = 5$, isomer (cpl5) surface structure is the most stable, with the other isomers being considerably less stable than isomer (cpl5); (5) for $n = 6$, isomer (cpl6) surface structure is the most stable, with the other isomers being considerably less stable than isomer (cpl6).

For $\text{Cl}^-(\text{H}_2\text{O})_n$ ($n = 2-6$) clusters, our prediction for the most stable isomers agrees with the results shown in refs 10, 25, 41. For the $\text{F}^-(\text{H}_2\text{O})_2$ cluster, isomer (2) is the most stable. For the $\text{F}^-(\text{H}_2\text{O})_3$ cluster, isomer (3) is the most stable, with isomers (4) and (5) being less stable than isomer (3) by 1.2–1.4 kcal/mol. For the $\text{F}^-(\text{H}_2\text{O})_4$, $\text{F}^-(\text{H}_2\text{O})_5$, and $\text{F}^-(\text{H}_2\text{O})_6$ clusters, isomer (6) surface structure, isomer (17) surface structure, and isomers (22) surface structure and (24) internal structure are the most stable, respectively.

The cause of the difference between the stability of the isomers for the $\text{Cl}^-(\text{H}_2\text{O})_n$ and $\text{F}^-(\text{H}_2\text{O})_n$ clusters is as follows. The interaction between Cl^- and water molecules is much

weaker than that between F^- and water molecules. Further, the conformation of the $\text{Cl}^-(\text{H}_2\text{O})_n$ isomers is very much different from that of the corresponding $\text{F}^-(\text{H}_2\text{O})_n$ isomers.

For $\text{Cl}^-(\text{H}_2\text{O})_n$ at 298 K, Table 3 shows that: (1) for $n = 2$, isomer (2') is considerably more stable than isomer (cpl2); (2) for $n = 3$, isomers (3'), (4'), and (5') are the most stable; (3) for $n = 4$, isomers (10') surface structure, (12') surface structure, and (14') surface structure are the most stable; (4) for $n = 5$, isomer (19') internal structure is the most stable, with the other isomers being considerably less stable than isomer (19'); (5) for $n = 6$, isomer (27') internal structure is the most stable, with the other isomers being considerably less stable than isomer (27').

At the MP4/6-311++G(2d,2p)//MP2/6-31++G(2d,2p) level, the $-\Delta H_{n-1,n}^{298\text{K}}$ ($n = 1-6$) of the minimum energy conformers [(1'), (cpl2), (3'), (9'), (cpl5), (cpl6)] are 15.1, 13.8, 14.4, 12.3, 10.8, and 13.3 kcal/mol, while $-\Delta H_{n-1,n}^{298\text{K}}$ ($n = 1-6$) of the conformers [(1'), (2'), ((3'), (4') and (5')), ((10'), (12') and (14')), (19'), (27')] are 15.1, 14.1, 12.8, 11.8, 10.7, and 8.7 kcal/mol. The latter conformers are in better agreement with the experimental $-\Delta H_{n-1,n}^0$ values⁴² (14.7, 13.0, 11.8, 10.6, 9.5, and 8.8). This indicates that the latter conformers are more populated than the former conformers at room temperature.

According to ref 23 for $\text{F}^-(\text{H}_2\text{O})_n$ at 298 K, for $n = 2$, isomer (2) is the most stable. For $n = 3$, isomer (3) is the most stable. For $n = 4$, isomer (14) internal structure is most stable. For $n = 5$, isomer (18) internal structure is most stable. For $n = 6$, isomer (24) internal structure is most stable.

The relative stability of the $\text{Cl}^-(\text{H}_2\text{O})_n$ isomers is much different from that of the corresponding $\text{F}^-(\text{H}_2\text{O})_n$ isomers at

TABLE 5: Shift of the OH Harmonic Frequencies for Cl⁻(H₂O)_n (n = 1–6) Clusters at the MP2/6-31++G(2d,2p) Level^a

1'	$\delta\omega$	intensity	2'	$\delta\omega$	intensity	19'	$\delta\omega$	intensity	20'	$\delta\omega$	intensity
	-525	1059		-441	291		-294	704		-317	177
	+9	35		-402	1122		-286	15		-298	430
				-19	73		-252	346		-228	93
				-17	28		-250	328		-221	205
cpl2	$\delta\omega$	intensity	3'	$\delta\omega$	intensity		-227	17		-176	205
	-576	673		-322 [2]	122		-185	54		-161	283
	-258	400		-294	772		-176	252		-141	241
	-99	163		-114	242		-173	200		-110	199
	0	41		-127 [2]	168		-151	619		-92	201
4'	$\delta\omega$	intensity	5'	$\delta\omega$	intensity		+15	59		-53	108
	-550	758		-551	761	21'	$\delta\omega$	intensity	28'	$\delta\omega$	intensity
	-506	1191		-507	1197		-245	49		-628	947
	-252	237		-253	237		-237 [2]	321		-300	284
	-174	481		-177	482		-226 [2]	0		-276	166
	0	27		-3	77		-156 [2]	0		-251	108
	1	67		-2	21		-156 [2]	424		-189	501
6'	$\delta\omega$	intensity	7'	$\delta\omega$	intensity		-139	628		-180	394
	-547	631		-565	926					-169	340
	-503	1071		-330	411					-118	173
	-280	256		-302	201					-58	154
	-215	169		-272	108					-11	55
	-196	493		-210	606	29'	$\delta\omega$	intensity	cpl6	$\delta\omega$	intensity
	-125	362		-174	432		-392	977		-621	886
	+2	14		-134	183		-341	279		-408	38
	+3	84		-1	51		-283	22		-357	721
8'	$\delta\omega$	intensity	9'	$\delta\omega$	intensity		-263	161		-319	496
	-665	1221		-276	139		-254	190		-283	236
	-524	1034		-267 [2]	199		-227	360		-282	371
	-286	325		-259	0		-182	324		-233	334
	-197	372		-184	371		-172	438		-201	20
	-176	219		-180	9		-128	180		-179	311
	-80	205		-176	9		+17	55		-166	731
	-1	51								-85	153
	+3	51								+2	58
10'	$\delta\omega$	intensity	11'	$\delta\omega$	intensity	22'	$\delta\omega$	intensity	23'	$\delta\omega$	intensity
	-551	873		-597	941		-494	746		-406	561
	-341	413		-448	894		-459	1010		-359	242
	-308	206		-235	238		-351	632		-298	503
	-279	139		-192	239		-218	183		-280	120
	-210	606		-147	410		-205	254		-252	123
	-186	479		-69	160		-153	169		-220	81
	-106	138		-6	50		-128	397		-209	623
	-6	52		+1	56		-113	327		-179	591
12'	$\delta\omega$	intensity	13'	$\delta\omega$	intensity		-59	195		-167	132
	-603	945		-599	719		-8	79		-131	192
	-449	888		-548	1554		-6	58		-52	173
	-234	241		-441	916		+3	61		-6	66
	-202	262		-324	170	24'	$\delta\omega$	intensity	25'	$\delta\omega$	intensity
	-148	397		-269	718		-600	867		-584	926
	-70	157		-1	36		-447	690		-371	267
	-4	62		0	65		-330	472		-354	351
	-2	46		+16	45		-292	115		-300	579
							-267	219		-279	168
							-235	255		-213	517
14'	$\delta\omega$	intensity	15'	$\delta\omega$	intensity		-209	520		-203	288
	-359	277		-442	901		-167	323		-178	157
	-312	392		-372	355		-140	370		-131	170
	-254	243		-345	437		-106	304		-110	175
	-198	260		-289	394		-9	67		-67	246
	-151	258		-182	271		0	58		+5	59
	-134	192		-139	201	26'	$\delta\omega$	intensity	27'	$\delta\omega$	intensity
	-79	32		-71	95		-612	887		-358	393
	-67	216		+14	52		-341	389		-333	1131
16'	$\delta\omega$	intensity	cpl5	$\delta\omega$	intensity		-274	217		-235	75
	-420	922		-409	385		-246	467		-224	169
	-355	435		-342	341		-232	77		-214	117
	-342	297		-337	433		-215	162		-194	140
	-298	444		-274	438		-162	365		-141	387
	-186	287		-252	48		-154	380		-137	209
	-136	190		-186	339		-111	224		-133	171
	-81	108		-158	389		-79	236		-124	467
	21	52		-147	273		-76	140		+2	100
				-105	149		+2	61		+4	37
				-40	88						
17'	$\delta\omega$	intensity	18'	$\delta\omega$	intensity						
	-544	848		-388	665						
	-420	1260		-336	444						
	-385	363		-250	94						
	-227	83		-244	296						
	-225	377		-224	199						
	-143	498		-151	423						
	-128	317		-138	77						
	-8	61		-131	385						
	-1	76		-94	154						
	+2	43		+1	62						

^a The shifts are given with respect to the corresponding mean of the symmetric and asymmetric OH stretch in water (3913 cm⁻¹). The frequency shifts are given in cm⁻¹ and the IR intensities in km/mol. The numbers in square brackets denote degeneracy.

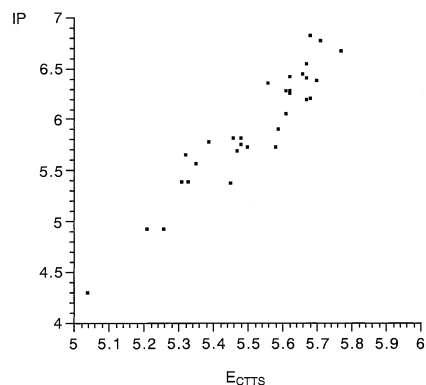


Figure 10. A plot of IP vs. E_{CTTS} for $\text{Cl}^-(\text{H}_2\text{O})_n$ using MP2/6-31++G-(2d,2p) results.

298 K. The relative stability of the $\text{Cl}^-(\text{H}_2\text{O})_n$ isomers at 298 K is different from that at 0 K, because of the entropy effect.

We have represented the vertical ionization potentials of Cl^- and the $\text{Cl}^-(\text{H}_2\text{O})_n$ cluster as $\text{IP}_v(\text{Cl}^-)$ and $\text{IP}_v[\text{Cl}^-(\text{H}_2\text{O})_n]$, respectively, and the integral shift $\text{dIP}_v(n)$ and the differential shifts $\text{DIP}_v(n)$ for the n th $\text{Cl}^-(\text{H}_2\text{O})_n$ cluster are represented by $\text{dIP}_v(n) = \text{IP}_v[\text{Cl}^-(\text{H}_2\text{O})_n] - \text{IP}_v(\text{Cl}^-)$ and $\text{DIP}_v(n) = \text{IP}_v[\text{Cl}^-(\text{H}_2\text{O})_n] - \text{IP}_v[\text{Cl}^-(\text{H}_2\text{O})_{n-1}]$, respectively.

The values for IP_v , dIP_v , and DIP_v obtained from Koopman's theorem from MP2 calculations are shown in Table 4. As the vertical ionization potentials for one isomers are close to those for the other isomers, stable isomers cannot be identified by use of the vertical ionization potentials, although the calculated vertical ionization potentials for the isomers are close to the observed experimental values.

We have also considered the energy band gap or the ionization potential at the situation of the CTTS system (E_{CTTS}).⁵⁴ An empirical estimate of this energy is obtained by

$$E_{\text{CTTS}} = E[\text{Cl}^-(\text{H}_2\text{O})_n] - E[\text{Cl}] - E[(\text{H}_2\text{O})_{n-1}^-]$$

This energy is also listed in Table 4. Figure 10 shows the linear relationship of IP with E_{CTTS} . A similar trend has been found for $\text{F}^-(\text{H}_2\text{O})_n$.²³

Table 4 shows that the charge transfer from Cl^- to $(\text{H}_2\text{O})_n$ in $\text{Cl}^-(\text{H}_2\text{O})_n$ increases with cluster size. A similar trend has been found for $\text{F}^-(\text{H}_2\text{O})_n$.²³ The charge transfer in $\text{Cl}^-(\text{H}_2\text{O})_n$ is slightly smaller than that in $\text{F}^-(\text{H}_2\text{O})_n$.

Table 5 shows the shift of the OH harmonic frequencies for $\text{Cl}^-(\text{H}_2\text{O})_n$. These results are useful for the identification of isomers using vibrational spectroscopy.

Fully optimized structural parameters are available free from the author.

IV. Conclusions

From this work we draw the following conclusions. (1) The structures of various $\text{Cl}^-(\text{H}_2\text{O})_n$ isomers differ considerably from those of the corresponding $\text{F}^-(\text{H}_2\text{O})_n$ isomers for $n = 2$ and 4–6, and especially so for $n = 6$. (2) The relative stability of the $\text{Cl}^-(\text{H}_2\text{O})_n$ isomers is markedly different from that of the corresponding $\text{F}^-(\text{H}_2\text{O})_n$ isomers at 0 and 298 K. For $\text{Cl}^-(\text{H}_2\text{O})_n$, the lowest energy structures for $n = 1$ –6 are predicted to be (1'), (cpl2), (3'), (9'), (cpl5), and (cpl6), respectively at 0 K, and the most stable isomers of the isomers for $n = 1$ –6 are predicted to be (1'), (2'), (3',4',5'), (10',12',14'), (19'), and (27'), respectively at 298 K. For $\text{F}^-(\text{H}_2\text{O})_n$, the lowest energy structures for $n = 1$ –6 are predicted to be (1), (2), (3), (6), (17), and (22, 24), respectively at 0 K, and the

most stable isomers of the isomers for $n = 1$ –6 are predicted to be (1), (2), (3), (14), (18), and (24), respectively at 298 K. (3) The relative stability of the $\text{Cl}^-(\text{H}_2\text{O})_n$ isomers at 298 K is very different from that at 0 K owing to the entropy effect. (4) The calculated vertical ionization potentials for the isomers are in close agreement with experimental values. However, since the vertical ionization potentials for one isomers are close to those for the other isomers, stable isomers cannot be identified by means of their vertical ionization potentials. (5) Our results for the E_{CTTS} and vibrational spectral characteristics of these clusters will be useful in future experimental investigations.

Acknowledgment. We are grateful to the Research Center for Computational Science for the use of the mainframe computer, and the Gaussian 94 and Gaussian 98 programs.

References and Notes

- (1) (a) Marcus, Y. *Ion Solvation*; Wiley-Interscience: New York, 1985. (b) Kirk, K. L. *Biochemistry of Halogens and Inorganic halides*; Plenum: New York, 1991.
- (2) Markovich, G.; Pollack, S.; Giniger, R.; Cheshnovsky, O. *J. Chem. Phys.* **1991**, *95*, 9416.
- (3) Markovich, G.; Pollack, S.; Giniger, R.; Cheshnovsky, O. *J. Chem. Phys.* **1994**, *101*, 9344.
- (4) Combariza, J. E.; Kestner, N. R.; Jortner, J. *J. Chem. Phys.* **1994**, *100*, 2851.
- (5) Combariza, J. E.; Kestner, N. R.; Jortner, J. *J. Chem. Phys. Lett.* **1993**, *203*, 423.
- (6) Makov, G.; Nitzan, A. *J. Phys. Chem.* **1994**, *98*, 3459.
- (7) Combariza, J. E.; Kestner, N. R. *J. Phys. Chem.* **1994**, *98*, 3513.
- (8) Xantheas, S. S.; Dunning, T. H., Jr. *J. Phys. Chem.* **1994**, *98*, 13489.
- (9) Xantheas, S. S. *J. Chem. Phys.* **1994**, *100*, 7523.
- (10) Xantheas, S. S. *J. Phys. Chem.* **1996**, *100*, 9703.
- (11) Xantheas, S. S.; Dang, L. X. *J. Phys. Chem.* **1996**, *100*, 3989.
- (12) Bryce, R. A.; Vincent, M. A.; Malcom, N. O.; Hiller, I. H.; Burton, N. A. *J. Chem. Phys.* **1998**, *109*, 3077.
- (13) Perera, L.; Berkowitz, M. L. *J. Chem. Phys.* **1991**, *95*, 1954.
- (14) Perera, L.; Berkowitz, M. L. *J. Chem. Phys.* **1993**, *99*, 4222.
- (15) Perera, L.; Berkowitz, M. L. *J. Chem. Phys.* **1994**, *100*, 3085.
- (16) Sremaniak, L. S.; Perera, L.; Berkowitz, M. L. *J. Chem. Phys. Lett.* **1994**, *218*, 377.
- (17) Yeh, I.-C.; Perera, L.; Berkowitz, M. L. *J. Chem. Phys. Lett.* **1997**, *264*, 31.
- (18) Dang, L. X.; Garrett, B. C. *J. Chem. Phys.* **1993**, *99*, 2972.
- (19) Gai, H.; Schenter, G. K.; Dang, L. X.; Garrett, B. C. *J. Chem. Phys.* **1996**, *105*, 8835.
- (20) Jorgensen, W. L.; Severance, D. L. *J. Chem. Phys.* **1993**, *99*, 4233.
- (21) Gao, J.; Gartner, D. S.; Jorgensen, W. L. *J. Am. Chem. Soc.* **1986**, *108*, 4784.
- (22) Truong, T. N.; Stefanovich, E. V. *J. Chem. Phys.* **1997**, *107*, 218.
- (23) Baik, J.; Kim, J.; Majumdar, D.; Kim, K. S. *J. Chem. Phys.* **1999**, *110*, 9116.
- (24) Lee, H. M.; Kim, K. S. *J. Chem. Phys.* **2001**, *114*, 4461.
- (25) Choi, J.-H.; Kuwata, K. T.; Cao, Y.-B.; Okumura, M. *J. Phys. Chem.* **1998**, *102*, 503.
- (26) Lybrand, T. P.; Kollman, P. A. *J. Chem. Phys.* **1985**, *83*, 2923.
- (27) Sung, S.-S.; Jordan, P. C. *J. Chem. Phys.* **1986**, *85*, 4045.
- (28) Lin, S.; Jordan, P. C. *J. Chem. Phys.* **1988**, *89*, 7492.
- (29) Dang, L. X.; Rice, J. E.; Caldwell, J.; Kollman, P. A. *J. Am. Chem. Soc.* **1991**, *113*, 2481.
- (30) Dang, L. X. *J. Chem. Phys.* **1992**, *97*, 2659.
- (31) Gai, H.; Dang, L. X.; Schenter, G. K.; Garrett, B. C. *J. Phys. Chem.* **1995**, *99*, 13303.
- (32) Perera, L.; Berkowitz, M. L. *J. Chem. Phys.* **1992**, *96*, 8288.
- (33) Perera, L.; Berkowitz, M. L. *Z. Phys. D* **1993**, *26*, 166.
- (34) Perera, L.; Berkowitz, M. L. *J. Chem. Phys.* **1993**, *99*, 4236.
- (35) Sremaniak, L. S.; Perera, L.; Berkowitz, M. L. *J. Phys. Chem.* **1996**, *100*, 1350.
- (36) Asada, T.; Nishimoto, K.; Kitaura, K. *J. Phys. Chem.* **1993**, *97*, 7724.
- (37) Asada, T.; Nishimoto, K.; Kitaura, K. *J. Mol. Struct.: THEOCHEM* **1994**, *310*, 149.
- (38) Stuart, S. J.; Berne, B. J. *J. Phys. Chem.* **1996**, *100*, 11934.
- (39) Okuno, Y. *J. Chem. Phys.* **1996**, *105*, 5817.
- (40) Dunbar, R. C.; McMahon, T. B.; Thölmann, D.; Tonner, D. S.; Salahub, D. R.; Wei, D. *J. Am. Chem. Soc.* **1995**, *117*, 12819.
- (41) Gora, R. W.; Roszak, S.; Leszczynski, J. *J. Chem. Phys. Lett.* **2000**, *325*, 7.

- (42) Hiraoka, K.; Mizuse, S.; Yamabe, S. *J. Phys. Chem.* **1988**, *92*, 3943.
- (43) Keesee, R. G.; Castleman, A. W., Jr. *Chem. Phys. Lett.* **1980**, *74*, 139.
- (44) Ashadi, M.; Yamdagni, R.; Kebarle, P. *J. Phys. Chem.* **1970**, *74*, 1475.
- (45) Frisch, M. J.; Trucks, G. W.; Schlegel, H. B.; Gill, P. M. W.; Johnson, B. G.; Robb, M. A.; Cheeseman, J. R.; Keith, T.; Petersson, G. A.; Montgomery, J. A.; Raghavachari, K.; Al-Laham, M. A.; Zakrzewski, V. G.; Ortiz, J. V.; Foresman, J. B.; Cioslowski, J.; Stefanov, B. B.; Nanayakkara, A.; Challacombe, M.; Peng, C. Y.; Ayala, P. Y.; Chen, W.; Wong, M. W.; Andres, J. L.; Replogle, E. S.; Gomperts, R.; Martin, R. L.; Fox, D. J.; Binkley, J. S.; Defrees, D. J.; Baker, J.; Stewart, J. P.; Head-Gordon, M.; Gonzalez, C.; Pople, J. A. *Gaussian 94*; Gaussian, Inc.: Pittsburgh, PA, 1995.
- (46) Frisch, M. J.; Trucks, G. W.; Schlegel, H. B.; Scuseria, G. E.; Robb, M. A.; Cheeseman, J. R.; Zakrzewski, V. G.; Montgomery, J. A., Jr.; Stratmann, R. E.; Burant, J. C.; Dapprich, S.; Millam, J. M.; Daniels, A. D.; Kudin, K. N.; Strain, M. C.; Farkas, O.; Tomasi, J.; Barone, V.; Cossi, M.; Cammi, R.; Mennucci, B.; Pomelli, C.; Adamo, C.; Clifford, S.; Ochterski, J.; Petersson, G. A.; Ayala, P. Y.; Cui, Q.; Morokuma, K.; Malick, D. K.; Rabuck, A. D.; Raghavachari, K.; Foresman, J. B.; Cioslowski, J.; Ortiz, J. V.; Stefanov, B. B.; Liu, G.; Liashenko, A.; Piskorz, P.; Komaromi, I.; Gomperts, R.; Martin, R. L.; Fox, D. J.; Keith, T.; Al-Laham, M. A.; Peng, C. Y.; Nanayakkara, A.; Gonzalez, C.; Challacombe, M.; Gill, P. M. W.; Johnson, B. G.; Chen, W.; Wong, M. W.; Andres, J. L.; Head-Gordon, M.; Replogle, E. S.; Pople, J. A. *Gaussian 98*; Gaussian, Inc.: Pittsburgh, PA, 1998.
- (47) Vaughn, S. J.; Akhmatskaya, E. V.; Vincent, M. A.; Masters, A. J.; Hiller, I. H. *J. Chem. Phys.* **1999**, *110*, 4338.
- (48) Masamura, M. *J. Comput. Chem.* **2001**, *22*, 31.
- (49) Boys, S. F.; Bernardi, F. *Mol. Phys.* **1970**, *19*, 553.
- (50) Xantheas, S. S. *J. Chem. Phys.* **1996**, *104*, 8821.
- (51) Masamura, M. *J. Chem. Phys.*, to be submitted.
- (52) Masamura, M.; Ikuta, S. *J. Comput. Chem.* **1999**, *20*, 1138.
- (53) Masamura, M. *J. Chem. Phys.*, in press.
- (54) (a) Serxner, D.; Dessent, C. E. H.; Johnson, M. A. *J. Chem. Phys.* **1996**, *105*, 7231. (b) Takahasi, N.; Sakurai, K.; Tanida, H.; Watanabe, I. *Chem. Phys. Lett.* **1995**, *246*, 183.
- (55) Klopper, W. *J. Chem. Phys.* **1995**, *102*, 6168.